

Radio pulse search from Aql X-1

LONG PENG,^{1,2} ZHAOSHENG LI,¹ YUANYUE PAN,¹ SHANSHAN WENG,³ WENMING YAN,^{2,4,5} NA WANG,^{2,4,5} BO-JUN WANG,⁶
AND SHUANGQIANG WANG^{2,7,4,5}

¹Key Laboratory of Stars and Interstellar Medium, Xiangtan University, Xiangtan 411105, Hunan, P.R. China

²Xinjiang Astronomical Observatory, Chinese Academy of Sciences, Urumqi, Xinjiang 830011, P.R. China

³Department of Physics and Institute of Theoretical Physics, Nanjing Normal University, Nanjing 210023, China

⁴Key Laboratory of Radio Astronomy, Chinese Academy of Sciences, Urumqi, Xinjiang, 830011, P.R. China

⁵Xinjiang Key Laboratory of Radio Astrophysics, Urumqi, Xinjiang, 830011, P.R. China

⁶National Astronomical Observatories, Chinese Academy of Sciences, Beijing 100101, China

⁷CSIRO Astronomy and Space Science, PO Box 76, Epping, NSW 1710, Australia

ABSTRACT

We present 12 observations of the accreting millisecond X-ray pulsar Aql X-1, taken from August 2022 to October 2023 using the Five-hundred-meter Aperture Spherical Radio Telescope at 1250 MHz. These observations covered both the quiescence and X-ray outburst states, as determined by analyzing the X-ray data from the Neutron Star Interior Composition Explorer and the Monitor of All-sky X-ray Image. Periodicity and single-pulse searches were conducted for each observation, but no pulsed signals were detected. The obtained upper limit flux densities are in the range of 2.86 – 5.73 μ Jy, which provide the lowest limits to date. We discuss several mechanisms that may prevent detection, suggesting that Aql X-1 may be in the radio-ejection state during quiescence, where the radio pulsed emissions are absorbed by the matter surrounding the system.

Keywords: Radio pulsars (1353); Millisecond pulsars (1062);

1. INTRODUCTION

Millisecond pulsars (MSPs) are a subclass of pulsars characterized by short rotation periods (e.g., < 30 ms) and low magnetic field strengths ($\sim 10^8$ G; see [Bhattacharya & van den Heuvel 1991](#); [Lorimer & Kramer 2004](#); [Manchester 2004](#); [Lorimer 2005](#); [Manchester 2017](#) for a review). The first MSP, PSR B1937+21, was discovered in 1982 by the Arecibo radio telescope ([Backer et al. 1982](#)). Shortly after the discovery of MSPs, the recycling scenario was proposed ([Alpar et al. 1982](#); [Radhakrishnan & Srinivasan 1982](#)). In this model, pulsars are spun up to millisecond periods by accreting matter and angular momentum from a companion star in low-mass X-ray binaries (LMXBs). During the accretion process, the neutron star is detectable as an X-ray source, known as an accreting millisecond X-ray pulsar (AMXP). When the companion star decouples from its Roche lobe, accretion in the AMXP ceases, as does the X-ray emission generated by mass trans-

fer. At this stage, the radio emission from the MSP becomes active. According to the recycling scenario, some LMXBs should host neutron stars with millisecond rotation periods. Until 1998, [Wijnands & van der Klis \(1998\)](#) provided the first confirmation of the recycling scenario by detecting coherent pulsations with a period of 2.5 ms in the LMXB SAX J1808.4–3658. The recycling scenario has been further supported by the discovery of transitional MSPs (tMSPs), which transition between rotation-powered and accretion-powered states, thereby bridging the gap between radio MSPs and AMXPs ([Archibald et al. 2009](#); [Papitto et al. 2013a](#); [Bassa et al. 2014a](#)).

More than 20 AMXPs have been discovered since the first detection of SAX J1808.4–3658 ([Wijnands & van der Klis 1998](#); [Di Salvo & Sanna 2020](#); [Patruno & Watts 2021](#)). AMXPs are typically X-ray transients, with X-ray luminosities of $\sim 10^{36} - 10^{37}$ ergs⁻¹ during outbursts, separated by extended quiescent periods at $L_X \sim 10^{31} - 10^{32}$ ergs⁻¹ (e.g., see [Patruno & Watts 2021](#) for a review). According to the recycling scenario, AMXPs are expected to behave as rotation-powered radio MSPs during X-ray quiescence and as accretion-

powered X-ray MSPs during outburst states (Campana et al. 1998a). However, no radio pulsed emissions have been detected during the quiescence of AMXPs, including sources such as Aql X-1 (Burgay et al. 2003), XTE J0929–314 (Iacolina et al. 2009), XTE J1751–305, XTE J1814–338, and SAX J1808.4–3658 (Iacolina et al. 2010). Burderi et al. (2001) proposed the radio-ejection model, in which an active radio pulsar during quiescence ejects accreting material from the system due to the pressure of its emission. However, the pulsar’s radio emissions are undetectable because of absorption by surrounding material, and searching for radio pulses at higher frequencies is suggested. Alternatively, for systems with long orbital periods, the ejected matter is spread over a wide orbit, which may reduce the amount of free-free absorption, increasing the likelihood of radio detection (Di Salvo & Sanna 2020).

Aql X-1 was discovered in 1965 (Friedman et al. 1967), with an orbital modulation of 18.95 hours and an orbital inclination of 36–47 degrees (Chevalier & Ilovaisky 1991; Welsh et al. 2000). Its distance is estimated to be between 4.0 and 5.75 kpc (Li et al. 2017). The optical counterpart of Aql X-1, designated as V1333 Aql, was identified in 1978 (Thorstensen et al. 1978). Aql X-1 is an intermittent AMXP, with coherent pulsations at a frequency of 550.273(1) Hz detected for only 120 seconds during a total exposure time of 1645 ks (Casella et al. 2008). Since its discovery, Aql X-1 has undergone multiple outbursts, approximately once a year, typically lasting from weeks to months (Degenaar et al. 2019).

The radio counterpart of Aql X-1 has been detected during some outbursts (e.g., Tudose et al. 2009; Miller-Jones et al. 2010; Díaz Trigo et al. 2018; Motta et al. 2019). Searches for radio pulsed emissions have been conducted using the 76-m Lovell Telescope at 925 MHz (Biggs & Lyne 1996) and the Parkes 64-m radio telescope at 1.4 GHz (Burgay et al. 2003), but no pulsed signals were detected, with upper flux density limits of a few mJy.

Due to its high sensitivity, the Five-hundred-meter Aperture Spherical radio Telescope (FAST; Nan et al. 2011) is an ideal instrument for searching for radio pulsed emissions from AMXPs. Here, we report on a search for radio pulsed emissions from Aql X-1 using FAST. We also note that Aql X-1 has a longer orbital period of 19 hours compared to other AMXPs (Di Salvo & Sanna 2020), which may increase the likelihood of detection according to the radio-ejection model (Burderi et al. 2001). In Section 2, we introduce the observations and data processing methods. In Section 3, we present the results of the radio pulse search. In Section 4, we discuss and summarize our findings.

2. OBSERVATIONS AND DATA PROCESSING

2.1. FAST Observations

We conducted 12 observations of Aql X-1 with FAST, two in 2022 and ten in 2023 (Table 1). These observations were used the central beam of the 19-beam receiver, covering a frequency range of 1.05–1.45 GHz, with a central observing frequency of 1.25 GHz (Jiang et al. 2020). The data were recorded in the PSR-FITS format (Hotan et al. 2004), with 8-bit resolution, 4096 frequency channels, each having a bandwidth of 0.122 MHz, four polarizations, and a sampling interval of 49.152 μ s.

2.2. Periodicity Search

We carried out blind periodic searches for the observations of Aql X-1 with FAST using the PRESTO software package¹ (Ransom 2001). For each observation, we used `rfifind` to identify radio frequency interference (RFI) in both the time and frequency domains and to generate an RFI mask. We then determined the range of trial dispersion measures (DMs) for searching Aql X-1. The observed width of a radio pulse is influenced by propagation effects and signal-processing response times (Cordes & McLaughlin 2003), and can be expressed as:

$$W_{\text{obs}} = \sqrt{W_{\text{int}}^2 + t^2 + t_{\text{DM}}^2 + t_{\text{scatt}}^2}, \quad (1)$$

where W_{int} is the intrinsic pulse width, t is the time resolution of the receiver, t_{DM} is the pulse broadening due to smearing across individual frequency channels, and t_{scatt} is the broadening due to interstellar scattering. For our observations with FAST, t is small and can be neglected. Both t_{DM} and t_{scatt} depend on the DM. The t_{DM} is given by:

$$t_{\text{DM}} = 8.3 \mu\text{s DM } \Delta\nu_{\text{MHz}} \nu_{\text{GHz}}^{-3}, \quad (2)$$

where ν_{MHz} and $\Delta\nu_{\text{MHz}}$ are the central observing frequency and bandwidth of an individual frequency channel, respectively. The t_{scatt} can be expressed as (Cordes 2002):

$$\log t_{\text{scatt}} = -3.72 + 0.411 \log \text{DM} + 0.937(\log \text{DM})^2 - 4.4 \log \nu_{\text{GHz}} \mu\text{s}. \quad (3)$$

The rotation period of Aql X-1 has been determined in the X-ray waveband as 1.8 ms (Casella et al. 2008). For our observations, $\nu = 1.25$ GHz and $\Delta\nu = 0.122$ MHz. For a DM of 500 pc cm⁻³, we found $t_{\text{DM}} = 0.26$ ms,

¹ <https://github.com/scottransom/presto>

Table 1. Details of FAST Observation and Data Reduction

Obs.No.	Obs. Date	Obs. MJD	Length (hr)	Orbital phase	z_{\max}	$z_{\max}^{(a)}$	State	Sensitivity (μJy)
01	2022-08-31	59822.50	2.0	0.51 - 0.60	430	600	q	2.86
02	2022-09-29	59851.46	1.0	0.18 - 0.23	108	200	q	4.05
03	2023-06-20	60114.76	1.0	0.68 - 0.79	108	200	q	4.05
04	2023-07-02	60126.73	1.0	0.85 - 0.90	108	200	q	4.05
05	2023-07-18	60143.63	1.3	0.26 - 0.33	191	200	q	3.51
06	2023-08-26	60182.59	0.5	0.60 - 0.63	27	100	o	5.73
07	2023-09-02	60189.51	0.5	0.37 - 0.40	27	100	o	5.73
08	2023-09-09	60196.59	0.5	0.33 - 0.36	27	100	o	5.73
09	2023-09-16	60203.50	0.5	0.09 - 0.11	27	100	o	5.73
10	2023-09-24	60211.44	0.5	0.14 - 0.17	27	100	q	5.73
11	2023-10-01	60218.42	0.5	0.98 - 0.01	27	100	q	5.73
12	2023-10-21	60238.38	0.5	0.27 - 0.30	27	100	q	5.73

Column (1) Observation number, (2) Observation date, (3) Observation Modified Julian Date (MJD), (4) Observation duration, (5) Orbital phase, (6) Calculated z_{\max} value, (7) Actual z_{\max} value used in accelerated search, (8) The outburst (o) or quiescent (q) state. (9) Upper limit flux density.

which is negligible, and $t_{\text{scatt}} = 6.14$ ms, which is several times of the rotation period of Aql X-1. We arbitrary set the maximum trial DM in our search to 500 pc cm^{-3} . Note that the estimated DM of Aql X-1 is 147 pc cm^{-3} , based on the YMW16 electron density model (Yao et al. 2017).

We used the procedure `DDplan.py` to determine near-optimal de-dispersion methods, setting DM steps of 0.05 pc cm^{-3} and 0.1 pc cm^{-3} for DMs from 0–370 pc cm^{-3} and 370–500 pc cm^{-3} , respectively. The `prepsubband` tool was used to de-disperse subbands, and `realfft` performed a discrete Fourier transform (DFT) on the de-dispersed time series. Since Aql X-1 is in a binary system, we used `accelsearch` to conduct Fourier-domain acceleration searches.

The z_{\max} parameter, which defines the maximum number of Fourier bins that the highest harmonic can drift linearly in the power spectrum (Ransom 2001), is calculated as:

$$z_{\max} = \frac{a_{\max} T^2 f_0}{c}, \quad (4)$$

where T is the total integration time, f_0 is the pulsar’s spin frequency, a_{\max} is the maximum orbital acceleration, and c is the speed of light. The calculated z_{\max} for each observation is shown in the sixth column of Table 1. Note that the actual z_{\max} may be larger, as Eq. 5 does not account for the eccentricity of the binary orbit. The values of z_{\max} used in our search are provided in the seventh column of Table 1.

The a_{\max} is derived using Kepler’s Third Law:

$$a_{\max} = \left(\frac{2\pi}{P_{\text{orb}}} \right)^{4/3} (T_{\odot} f)^{1/3} c, \quad (5)$$

where P_{orb} is the orbital period, $T_{\odot} = GM_{\odot}/c^3 = 4.925490947 \mu\text{s}$, and f is the mass function, defined as:

$$f = \frac{4\pi^2}{G} \frac{x^3}{P_{\text{orb}}^2} = \frac{(m_c \sin i)^3}{(m_p + m_c)^2}. \quad (6)$$

Using X-ray reflection modeling, the orbital inclination i is constrained to $(26 \pm 2)^\circ$ (Ludlam et al. 2017), and assuming the pulsar mass m_p to be $1.4 M_{\odot}$ (Thorsett & Chakrabarty 1999), we calculate $a_{\max} = 4.52 \text{ m/s}^2$.

We used `ACCEL_sift.py` to reject bad candidates and combine detections of the same candidate. We also employed `Jinglepulsar`² for more sensitive detection of faint signals (Pan et al. 2021). For each candidate, we folded the raw data using `prepfold`, generating diagnostic plots that were inspected manually.

2.3. Single-pulse Search

To search for single-pulses, the de-dispersed time series was analyzed using the `single_pulse_search.py`. The trial DM and DM steps used for single-pulse search were the same as those for the periodicity search. We identified single-pulse candidates with a signal-to-noise ratio (S/N) greater than 7 and folded the raw data according to the DM of each candidate using the `dspsr` software (van Straten & Bailes 2011). Frequency-time plots were then generated for the candidates, which were visually inspected to confirm their validity.

2.4. X-ray Observations

We noted that Aql X-1 exhibited X-ray outbursts during 2022 and 2023, which were detected by the Neu-

² <https://www.github.com/jinglepulsar>

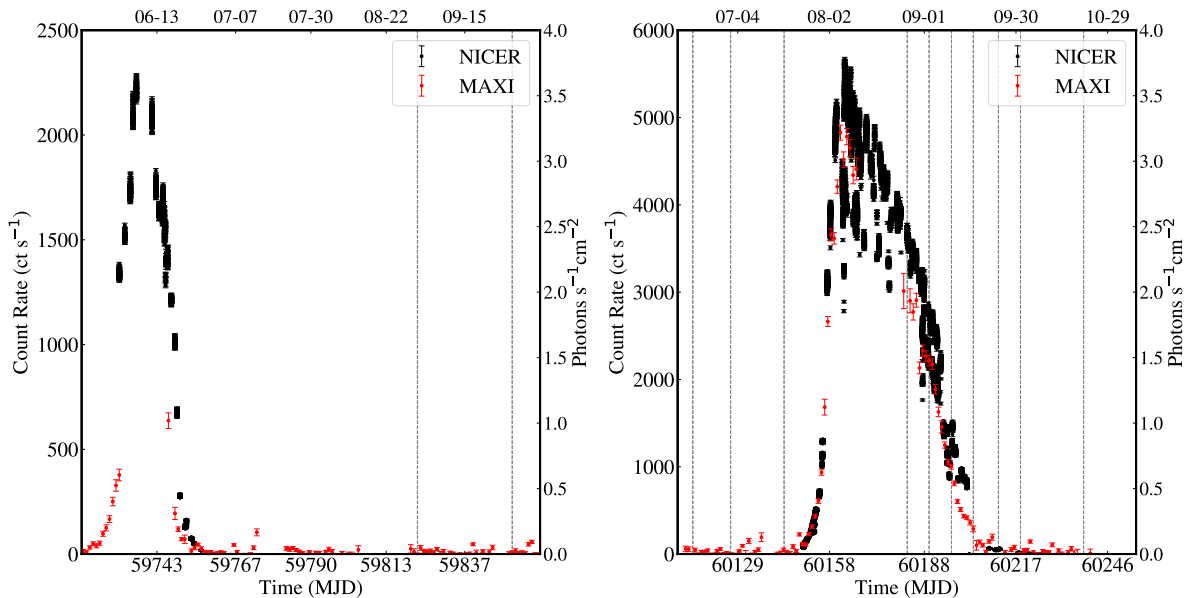


Figure 1. The left and right panels display the X-ray light curves of Aql X-1 for the years 2022 and 2023, respectively. Black dots: NICER background-subtracted light curves in units of ct s^{-1} (0.5–10.0 keV, 16 s resolution). Red dots: MAXI light curves in units of $\text{Photons s}^{-1} \text{cm}^{-2}$ (2–20 keV, 1 day resolution). The gray dashed vertical lines indicate the MJDs of the FAST observations conducted in 2022 and 2023.

tron Star Interior Composition Explorer (NICER) (Alabarta et al. 2023b,c,a; Homan et al. 2023). To determine the precise time spans of the X-ray outburst and quiescence states, we retrieved the available NICER observational data for Aql X-1 from 2022 and 2023 through the High Energy Astrophysics Science Archive Research Center (HEASARC)³. The data were processed using HEASOFT 6.31.1 and NICER Data Analysis Software (NICERDAS), applying standard filtering criteria for routine NICERL2 to extract cleaned event data. The light curves of X-ray emission, binned at 16 seconds, were obtained using the NICERL3-LC pipeline. We also retrieved the observational data of the Monitor of All-sky X-ray Image (MAXI), and obtained the 2–20 keV light curve data with a bin size of 1 day from MAXI/GSC⁴.

3. RESULTS

In Figure 1, we present the light curves for Aql X-1 observed by NICER and MAXI between 2022 and 2023, with high and low backgrounds subtracted. The observations with FAST are marked as vertical dotted lines, covering both the X-ray burst and quiescence states. Using the ephemerides of

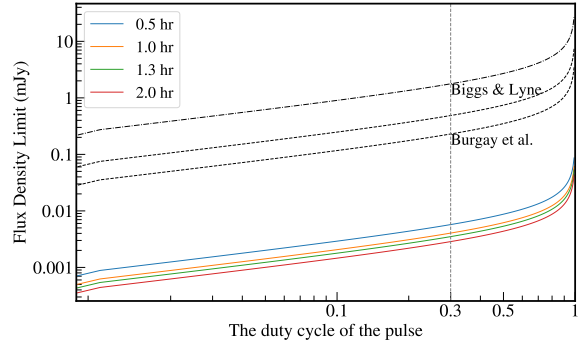


Figure 2. The upper limit flux density for Aql X-1 as a function of the duty cycle. Solid lines in different colors represent various integration times. The dot-dashed and dotted lines indicate the limits obtained by Biggs & Lyne (1996) and Burgay et al. (2003), respectively, with the flux densities scaled to 1250 MHz assuming a spectral index of -1.6 . The gray dashed line denotes the duty cycle of the pulse as utilized in our work.

Aql X-1 provided by Mata Sánchez et al. (2017), we calculated the orbital phase of each observation by assuming a circular orbit (see the fifth column of Table 1). Our observations span different orbital phases. We performed periodic and single-pulse searches for each observation, but no pulsed signals were detected.

³ <https://heasarc.gsfc.nasa.gov>

⁴ <http://maxi.riken.jp/mxondem/>

We estimated the upper limit of the flux density for each observation. For the periodicity search, the minimum detectable flux density is given by (Lorimer & Kramer 2004):

$$S_{\min} = \frac{(S/N)\beta T_{\text{sys}}}{G(n_p t_{\text{int}} \Delta F)^{1/2}} \left(\frac{W}{P - W} \right)^{1/2}, \quad (7)$$

where G is the telescope gain, T_{sys} is the system temperature, n_p is the number of polarizations, ΔF is the observational frequency bandwidth, β is the sensitivity degradation factor, W is the pulse width, P is the spin period, and S/N is the threshold signal-to-noise ratio required for detection. For FAST observations, the parameters are $G = 16$ K/Jy, $T_{\text{sys}} = 24$ K, $n_p = 2$, $\beta = 1$, and $\Delta F = 400$ MHz (Jiang et al. 2020).

As described in Section 2, the observed pulse width W_{obs} depends on the intrinsic pulse width, interstellar scattering, and smearing across individual frequency channels (Cordes & McLaughlin 2003). The effects of pulse smearing and the receiver’s time resolution are negligible, but t_{scatt} strongly depends on the DM. Figure 2 shows how the upper limit of the flux density varies with the pulse duty cycle, showing that the upper limit increases as the duty cycle increases. Assuming $W = 0.3P$, which is typical for MSPs, and $S/N = 7$, we estimated S_{\min} for each observation. The results, shown in the last column of Table 1, indicate that S_{\min} ranges from ~ 2.86 to 5.73 μJy , depending on the duration of each observation.

For the single-pulse search, the minimum detectable peak flux density is (Cordes & McLaughlin 2003):

$$S_{\min} = \frac{(S/N_{\text{peak}})2\beta T_{\text{sys}}}{G(n_p W \Delta F)^{1/2}}, \quad (8)$$

where S/N_{peak} is the peak signal-to-noise ratio of a pulse. Single-pulses from a given pulsar are typically unstable, exhibiting varying widths (e.g., Parthasarathy et al. 2021; Wang et al. 2024). Assuming a single-pulse width of $W = 0.3P$ (about 0.54 ms) and $S/N_{\text{peak}} = 7$, we derived an upper limit for the detectable peak flux density of 15.6 mJy. It should be noted that this value has significant uncertainty.

4. DISCUSSION AND CONCLUSIONS

We present radio observations of Aql X-1 during both X-ray outburst and quiescence states. No pulsed signals were detected by FAST through periodicity and single-pulse searches. The lowest upper limit on the flux density from our observations is ~ 2.86 μJy , assuming a pulse width of $W = 0.3P$. Previous searches for radio emission from Aql X-1 were conducted using the 76-m

Lovell Telescope at 925 MHz (Biggs & Lyne 1996) and the Parkes 64-m radio telescope at 1.4 GHz (Burgay et al. 2003), and no pulsed signals were detected. Note that at that time, the rotation period of Aql X-1 was not yet determined. Pulsars typically exhibit steep spectra that can be modeled by a simple power law (Sieber 1973). Using a mean spectral index of -1.6 (Lorimer et al. 1995), we estimated the implied upper limit flux densities for Aql X-1 using the same method from Biggs & Lyne (1996) and Burgay et al. (2003), as shown in Figure 2. Our results are more than ten times lower than previous limits.

For AMXPs, during X-ray outburst states, the magnetospheric radius is smaller than the corotation radius. In such cases, accretion matters reaches the neutron star surface, producing X-ray emission, and quenches the pulsar’s radio emission, making it undetectable (Patruno & Watts 2021). During quiescence, the radio pulsar is expected to be active according to the recycling scenario (Patruno & Watts 2021), supported by optical observations (Burderi et al. 2003). However, despite many searches, no radio pulsations have been detected in AMXPs (Burgay et al. 2003; Iacolina et al. 2009, 2010).

For Aql X-1 in quiescence, it is unclear whether the system is in the radio-ejection phase or the radio-pulsar phase. In the radio-pulsar phase, non-detection could arise from several factors: (1) the radio emission may be intrinsically too weak. However, Aql X-1’s distance of ~ 4.5 kpc is smaller than that of IGR J18245–2452 (~ 5.5 kpc) and comparable to other known radio MSPs, making this explanation less likely. (2) The radio beam may not sweep across Earth. Radio beams are generally narrower than X-ray beams in MSPs (see Lorimer 2008 for a review). Burgay et al. (2003) estimated that the average sky fraction swept by radio beams for MSPs is ~ 0.57 . Given that radio pulsations are detected in only one AMXP (IGR J18245–2452) among over 20 known AMXPs (Patruno & Watts 2021), this scenario is unlikely to be the primary cause of non-detection in a statistical sense. However, for Aql X-1, it is unknown whether the radio beam is pointed away from Earth. (3) The radio pulsed emission may be intermittent. In this scenario, the radio pulsed emission may occur at particular times or orbital phases. IGR J18245–2452 was sporadically detected as a faint radio pulsar with a flux density of $10 - 20$ μJy at 2 GHz (Bégin 2006; Papitto et al. 2013b). We conducted only 12 observations of Aql X-1, with a cadence ranging from several days to tens of days. This is insufficient to provide constraints on this scenario. Further observations with smaller cadences and longer durations are needed.

Table 2. L_X for tMSPs in different states

Name	Disc state			Rotation-powered state		Ref.
	$L_{X,\text{flare}}$	$L_{X,\text{high}}$	$L_{X,\text{low}}$	$L_{X,\text{rot}}$		
	10^{33} erg/s	10^{33} erg/s	10^{33} erg/s	10^{33} erg/s		
PSR J1023+0038	9.6(1)	2.85(4)	0.57(3)	0.16(5)		Archibald et al. (2015); Linares (2014)
XSS J12270–4859	9.6(1)	4.2(1)	0.64(1)	0.11(1)		Miraval Zanon et al. (2020)
IGR J18245–2452		3.9(1)	0.56(10)	0.22(4)		Linares et al. (2014)
		Propeller	Radio-ejection	Radio pulsar	Campana et al. (2016); Miraval Zanon et al. (2020)	

In the radio-ejection phase, the radio pulsar remains active but is undetectable due to absorption by surrounding material in the radio-ejection state (Burderi et al. 2001). The discovery of tMSPs has provided further insight into the behavior of AMXPs in quiescence (Archibald et al. 2009; Papitto et al. 2013a; Bassa et al. 2014b). TMSPs exhibit different X-ray modes during the disc state (Campana & Di Salvo 2018), as shown in Table 2. To explain the various modes of tMSPs during the disc state, Campana et al. (2016) proposed the propeller model, in which the inflowing disk matter is halted at the magnetospheric boundary, acting as a centrifugal barrier. According to this model, a small fraction of disk matter may leak through the centrifugal barrier (Campana et al. 2016) and reach the neutron star surface due to an advection-dominated accretion flow, where radiation is trapped within the disk (Narayan & Yi 1994). This process corresponds to the high mode of X-ray luminosity (Campana et al. 2016; Miraval Zanon et al. 2020). If the accretion rate decreases, the disc pressure diminishes, causing the magnetospheric radius to expand. When the magnetospheric radius reaches the light cylinder radius, the system transitions into the radio-ejection phase, where accreted matter is expelled, corresponding to the low mode of X-ray luminosity (Burderi et al. 2001; Campana et al. 2016). If the mass accretion rate decreases further, the system enters the radio pulsar state, where the corresponding X-ray luminosity is even lower (Campana et al. 2016). For Aql X-1, the quiescent X-ray luminosity, $L_X \sim 0.6 \times 10^{33} \text{ erg s}^{-1}$ (Campana et al. 1998b), is comparable to that of tMSPs in the low mode. By analyzing the X-ray luminosity and hard spectrum of Aql X-1 in quiescence, Campana et al. (1998b) suggested that its observational properties can be interpreted as shock emission from a reactivated rotation-powered pulsar. These phenomena collectively support the hypothesis that Aql X-1 is in the radio-ejection phase during quiescence. The radio pulsed emission of Aql X-1 could potentially be detected if the mass accretion rate decreases further in quiescence.

Burgay et al. (2003) investigated the surrounding matter under the assumption that Aql X-1 is in the radio-ejection phase during quiescence and found that radio pulses at 1.4 GHz could be easily absorbed by this material. However, the precise frequency at which the radio pulsed emission might become detectable remains uncertain due to the limited understanding of the surrounding matter’s properties. Future observations of AMXPs at higher frequencies could provide valuable insights into their nature, utilizing facilities such as the QTT (Wang et al. 2023), ALMA (Matthews et al. 2018), ngVLA, and SKA (Selina et al. 2018; Braun et al. 2019). If radio pulsed emissions are detected at high frequencies but not at low frequencies, this would serve as direct evidence supporting the radio-ejection model. Additionally, observations using radio arrays could help constrain the radio continuum flux, which is essential for advancing our understanding of the accretion processes in AMXPs.

ACKNOWLEDGMENTS

We thank the referee for the valuable comments, which improved our manuscript. We acknowledge the science research grants from the China Manned Space Project. This work is supported by the National Natural Science Foundation of China (No. 12288102, No. 12103042, No. 12203092, No. 12041304, No. 12273030, No. 12473041), the science and technology innovation Program of Hunan Province (No. 2024JC0001), the Major Science and Technology Program of Xinjiang Uygur Autonomous Region (No. 2022A03013-3), the National SKA Program of China (No. 2020SKA0120100), the National Key Research and Development Program of China (No. 2022YFC2205202, No. 2021YFC2203502), the Natural Science Foundation of Xinjiang Uygur Autonomous Region (No. 2022D01B71), the Tianshan Talent Training Program for Young Elite Scientists (No. 2023TSYCQNTJ0024). This work made use of the data from FAST (Five-hundred-meter Aperture Spherical radio Telescope) (<https://cstr.cn/31116.02.FAST>). FAST is a Chinese national mega-science facility, operated by National Astronomical Observatories, Chinese Academy of Sciences. The research is partly supported by the

Operation, Maintenance and Upgrading Fund for Astronomical Telescopes and Facility Instruments, budgeted from the Ministry of Finance of China (MOF) and administrated by the Chinese Academy of Sciences (CAS).

Software: PRESTO (Ransom 2001), DSPSR (van Straten & Bailes 2011), HEASOFT(v6.31.1) , NICER-DAS(v010a)

REFERENCES

- Alabarta, K., Homan, J., Russell, D. M., et al. 2023a, The Astronomer’s Telegram, 16284, 1
- Alabarta, K., Russell, D. M., Baglio, M. C., et al. 2023b, The Astronomer’s Telegram, 16147, 1
- . 2023c, The Astronomer’s Telegram, 16187, 1
- Alpar, M. A., Cheng, A. F., Ruderman, M. A., & Shaham, J. 1982, *Nature*, 300, 728, doi: [10.1038/300728a0](https://doi.org/10.1038/300728a0)
- Archibald, A. M., Stairs, I. H., Ransom, S. M., et al. 2009, *Science*, 324, 1411, doi: [10.1126/science.1172740](https://doi.org/10.1126/science.1172740)
- Archibald, A. M., Bogdanov, S., Patruno, A., et al. 2015, *ApJ*, 807, 62, doi: [10.1088/0004-637X/807/1/62](https://doi.org/10.1088/0004-637X/807/1/62)
- Backer, D. C., Kulkarni, S. R., Heiles, C., Davis, M. M., & Goss, W. M. 1982, *Nature*, 300, 615, doi: [10.1038/300615a0](https://doi.org/10.1038/300615a0)
- Bassa, C. G., Patruno, A., Hessels, J. W. T., et al. 2014a, *MNRAS*, 441, 1825, doi: [10.1093/mnras/stu708](https://doi.org/10.1093/mnras/stu708)
- . 2014b, *MNRAS*, 441, 1825, doi: [10.1093/mnras/stu708](https://doi.org/10.1093/mnras/stu708)
- Bégin, S. 2006, Master’s thesis, University of British Columbia, Canada
- Bhattacharya, D., & van den Heuvel, E. P. J. 1991, *PhR*, 203, 1, doi: [10.1016/0370-1573\(91\)90064-S](https://doi.org/10.1016/0370-1573(91)90064-S)
- Biggs, J. D., & Lyne, A. G. 1996, *MNRAS*, 282, 691, doi: [10.1093/mnras/282.2.691](https://doi.org/10.1093/mnras/282.2.691)
- Braun, R., Bonaldi, A., Bourke, T., Keane, E., & Wagg, J. 2019, Anticipated Performance of the Square Kilometre Array – Phase 1 (SKA1). <https://arxiv.org/abs/1912.12699>
- Burderi, L., Di Salvo, T., D’Antona, F., Robba, N. R., & Testa, V. 2003, *A&A*, 404, L43, doi: [10.1051/0004-6361:20030669](https://doi.org/10.1051/0004-6361:20030669)
- Burderi, L., Possenti, A., D’Antona, F., et al. 2001, *ApJL*, 560, L71, doi: [10.1086/324220](https://doi.org/10.1086/324220)
- Burgay, M., Burderi, L., Possenti, A., et al. 2003, *ApJ*, 589, 902, doi: [10.1086/374690](https://doi.org/10.1086/374690)
- Campana, S., Colpi, M., Mereghetti, S., Stella, L., & Tavani, M. 1998a, *A&A Rv*, 8, 279, doi: [10.1007/s001590050012](https://doi.org/10.1007/s001590050012)
- Campana, S., Coti Zelati, F., Papitto, A., et al. 2016, *A&A*, 594, A31, doi: [10.1051/0004-6361/201629035](https://doi.org/10.1051/0004-6361/201629035)
- Campana, S., & Di Salvo, T. 2018, in *Astrophysics and Space Science Library*, Vol. 457, *Astrophysics and Space Science Library*, ed. L. Rezzolla, P. Pizzochero, D. I. Jones, N. Rea, & I. Vidaña, 149, doi: [10.1007/978-3-319-97616-7_4](https://doi.org/10.1007/978-3-319-97616-7_4)
- Campana, S., Stella, L., Mereghetti, S., et al. 1998b, *ApJL*, 499, L65, doi: [10.1086/311357](https://doi.org/10.1086/311357)
- Casella, P., Altamirano, D., Patruno, A., Wijnands, R., & van der Klis, M. 2008, *ApJL*, 674, L41, doi: [10.1086/528982](https://doi.org/10.1086/528982)
- Chevalier, C., & Ilovaisky, S. A. 1991, *A&A*, 251, L11
- Cordes, J. M. 2002, in *Astronomical Society of the Pacific Conference Series*, Vol. 278, *Single-Dish Radio Astronomy: Techniques and Applications*, ed. S. Stanimirovic, D. Altschuler, P. Goldsmith, & C. Salter, 227–250
- Cordes, J. M., & McLaughlin, M. A. 2003, *ApJ*, 596, 1142, doi: [10.1086/378231](https://doi.org/10.1086/378231)
- Degenaar, N., Ootes, L. S., Page, D., et al. 2019, *MNRAS*, 488, 4477, doi: [10.1093/mnras/stz1963](https://doi.org/10.1093/mnras/stz1963)
- Di Salvo, T., & Sanna, A. 2020, arXiv e-prints, arXiv:2010.09005, doi: [10.48550/arXiv.2010.09005](https://doi.org/10.48550/arXiv.2010.09005)
- Díaz Trigo, M., Altamirano, D., Dinçer, T., et al. 2018, *A&A*, 616, A23, doi: [10.1051/0004-6361/201832693](https://doi.org/10.1051/0004-6361/201832693)
- Friedman, H., Byram, E. T., & Chubb, T. A. 1967, *Science*, 156, 374, doi: [10.1126/science.156.3773.374](https://doi.org/10.1126/science.156.3773.374)
- Homan, J., Alabarta, K., Russell, D. M., et al. 2023, The Astronomer’s Telegram, 16153, 1
- Hotan, A. W., van Straten, W., & Manchester, R. N. 2004, *PASA*, 21, 302, doi: [10.1071/AS04022](https://doi.org/10.1071/AS04022)
- Iacolina, M. N., Burgay, M., Burderi, L., Possenti, A., & di Salvo, T. 2009, *A&A*, 497, 445, doi: [10.1051/0004-6361/200810677](https://doi.org/10.1051/0004-6361/200810677)
- . 2010, *A&A*, 519, A13, doi: [10.1051/0004-6361/201014025](https://doi.org/10.1051/0004-6361/201014025)
- Jiang, P., Tang, N.-Y., Hou, L.-G., et al. 2020, *Research in Astronomy and Astrophysics*, 20, 064, doi: [10.1088/1674-4527/20/5/64](https://doi.org/10.1088/1674-4527/20/5/64)
- Li, Z., Falanga, M., Chen, L., Qu, J., & Xu, R. 2017, *ApJ*, 845, 8, doi: [10.3847/1538-4357/aa7d0b](https://doi.org/10.3847/1538-4357/aa7d0b)
- Linares, M. 2014, *ApJ*, 795, 72, doi: [10.1088/0004-637X/795/1/72](https://doi.org/10.1088/0004-637X/795/1/72)

- Linares, M., Bahramian, A., Heinke, C., et al. 2014, MNRAS, 438, 251, doi: [10.1093/mnras/stt2167](https://doi.org/10.1093/mnras/stt2167)
- Lorimer, D. R. 2005, Living Reviews in Relativity, 8, 7, doi: [10.12942/lrr-2005-7](https://doi.org/10.12942/lrr-2005-7)
- . 2008, Living Reviews in Relativity, 11, 8, doi: [10.12942/lrr-2008-8](https://doi.org/10.12942/lrr-2008-8)
- Lorimer, D. R., & Kramer, M. 2004, Handbook of Pulsar Astronomy, Vol. 4
- Lorimer, D. R., Yates, J. A., Lyne, A. G., & Gould, D. M. 1995, MNRAS, 273, 411, doi: [10.1093/mnras/273.2.411](https://doi.org/10.1093/mnras/273.2.411)
- Ludlam, R. M., Miller, J. M., Degenaar, N., et al. 2017, ApJ, 847, 135, doi: [10.3847/1538-4357/aa8b1b](https://doi.org/10.3847/1538-4357/aa8b1b)
- Manchester, R. N. 2004, Science, 304, 542, doi: [10.1126/science.1097649](https://doi.org/10.1126/science.1097649)
- . 2017, Journal of Astrophysics and Astronomy, 38, 42, doi: [10.1007/s12036-017-9469-2](https://doi.org/10.1007/s12036-017-9469-2)
- Mata Sánchez, D., Muñoz-Darias, T., Casares, J., & Jiménez-Ibarra, F. 2017, MNRAS, 464, L41, doi: [10.1093/mnras/464/L41](https://doi.org/10.1093/mnras/464/L41)
- Matthews, L. D., Crew, G. B., Doeleman, S. S., et al. 2018, PASP, 130, 015002, doi: [10.1088/1538-3873/aa9c3d](https://doi.org/10.1088/1538-3873/aa9c3d)
- Miller-Jones, J. C. A., Sivakoff, G. R., Altamirano, D., et al. 2010, ApJL, 716, L109, doi: [10.1088/2041-8205/716/2/L109](https://doi.org/10.1088/2041-8205/716/2/L109)
- Miraval Zanon, A., Campana, S., Ridolfi, A., D’Avanzo, P., & Ambrosino, F. 2020, A&A, 635, A30, doi: [10.1051/0004-6361/201936356](https://doi.org/10.1051/0004-6361/201936356)
- Motta, S. E., Williams, D., Fender, R., et al. 2019, The Astronomer’s Telegram, 13016, 1
- Nan, R., Li, D., Jin, C., et al. 2011, International Journal of Modern Physics D, 20, 989, doi: [10.1142/S0218271811019335](https://doi.org/10.1142/S0218271811019335)
- Narayan, R., & Yi, I. 1994, ApJL, 428, L13, doi: [10.1086/187381](https://doi.org/10.1086/187381)
- Pan, Z., Ma, X.-Y., Qian, L., et al. 2021, Research in Astronomy and Astrophysics, 21, 143, doi: [10.1088/1674-4527/21/6/143](https://doi.org/10.1088/1674-4527/21/6/143)
- Papitto, A., Ferrigno, C., Bozzo, E., et al. 2013a, Nature, 501, 517, doi: [10.1038/nature12470](https://doi.org/10.1038/nature12470)
- . 2013b, Nature, 501, 517, doi: [10.1038/nature12470](https://doi.org/10.1038/nature12470)
- Parthasarathy, A., Bailes, M., Shannon, R. M., et al. 2021, MNRAS, 502, 407, doi: [10.1093/mnras/stab037](https://doi.org/10.1093/mnras/stab037)
- Patruno, A., & Watts, A. L. 2021, in Astrophysics and Space Science Library, Vol. 461, Timing Neutron Stars: Pulsations, Oscillations and Explosions, ed. T. M. Belloni, M. Méndez, & C. Zhang, 143–208, doi: [10.1007/978-3-662-62110-3_4](https://doi.org/10.1007/978-3-662-62110-3_4)
- Radhakrishnan, V., & Srinivasan, G. 1982, Current Science, 51, 1096
- Ransom, S. M. 2001, PhD thesis, Harvard University, Massachusetts
- Selina, R. J., Murphy, E. J., McKinnon, M., et al. 2018, in Society of Photo-Optical Instrumentation Engineers (SPIE) Conference Series, Vol. 10700, Ground-based and Airborne Telescopes VII, ed. H. K. Marshall & J. Spyromilio, 107001O, doi: [10.1117/12.2312089](https://doi.org/10.1117/12.2312089)
- Sieber, W. 1973, A&A, 28, 237
- Thorsett, S. E., & Chakrabarty, D. 1999, ApJ, 512, 288, doi: [10.1086/306742](https://doi.org/10.1086/306742)
- Thorstensen, J., Charles, P., & Bowyer, S. 1978, ApJL, 220, L131, doi: [10.1086/182651](https://doi.org/10.1086/182651)
- Tudose, V., Fender, R. P., Linares, M., Maitra, D., & van der Klis, M. 2009, MNRAS, 400, 2111, doi: [10.1111/j.1365-2966.2009.15604.x](https://doi.org/10.1111/j.1365-2966.2009.15604.x)
- van Straten, W., & Bailes, M. 2011, PASA, 28, 1, doi: [10.1071/AS10021](https://doi.org/10.1071/AS10021)
- Wang, N., Xu, Q., Ma, J., et al. 2023, Science China Physics, Mechanics, and Astronomy, 66, 289512, doi: [10.1007/s11433-023-2131-1](https://doi.org/10.1007/s11433-023-2131-1)
- Wang, S. Q., Wang, N., Wang, J. B., et al. 2024, ApJ, 964, 6, doi: [10.3847/1538-4357/ad217b](https://doi.org/10.3847/1538-4357/ad217b)
- Welsh, W. F., Robinson, E. L., & Young, P. 2000, AJ, 120, 943, doi: [10.1086/301486](https://doi.org/10.1086/301486)
- Wijnands, R., & van der Klis, M. 1998, Nature, 394, 344, doi: [10.1038/28557](https://doi.org/10.1038/28557)
- Yao, J. M., Manchester, R. N., & Wang, N. 2017, ApJ, 835, 29, doi: [10.3847/1538-4357/835/1/29](https://doi.org/10.3847/1538-4357/835/1/29)